Inconsistencies in sulphur dioxide emissions from the Canadian oil sands and potential implications

Chris A. McLinden[1,2], Cristen L. F. Adams[3], Vitali Fioletov[1], Debora Griffin[1], Paul A. Makar[1], Xiaoyi Zhao[1], Andrew Kovachik[1,4], Nolan Dickson[1,4], Cassandra Brown[3], Nicolay Krotkov[5], Can Li[5,6], Nicolas Theys[7], Pascal Hedelt[8], and Diego G. Loyola[8]

[1] Environment and Climate Change Canada, Toronto, Canada.
[2] University of Saskatchewan, Department of Physics and Engineering Physics
[3] Resource Stewardship Division, Alberta Environment and Parks, Edmonton, Alberta, Canada
[4] University of Waterloo, Department of Physics,
[5] Laboratory for Atmospheric Chemistry and Dynamics, NASA Goddard Space Flight Center, Greenbelt, MD, USA.
[6] Earth System Science Interdisciplinary Center, University of Maryland College Park, MD USA
[7] Royal Belgian Institute for Space Aeronomy (BIRA-IASB), Brussels, Belgium
[8] Institut für Methodik der Fernerkundung (IMF), Deutsches Zentrum für Luft und Raumfahrt (DLR), Oberpfaffenhofen, Germany

To be submitted to *Environment Research Letters*

Keywords: satellite remote sensing, SO2, emissions, oil sands, OMI, TROPOMI

Abstract.

Satellite-derived and reported sulphur dioxide (SO_2) emissions from the Canadian oil sands are shown to have been consistent up to 2013. Post-2013, these sources of emissions data diverged, with reported emissions dropping by a factor of two, while satellite-derived emissions for the region remained relatively constant, with the discrepancy (satellite-derived emissions minus reported emissions) peaking at 50 kT(SO_2) yr^{-1} around 2016. The 2013-2014 period corresponds to when new flue-gas desulphurization units came on-line. Previous work has established a high level of consistency between at-stack SO_2 emissions observations and satellite estimates, and surface monitoring network SO_2 concentrations over the same multi-year period show similar trends as the satellite data, with a slight increase in concentrations post-2013. No clear explanation for this discrepancy currently exists. The implications of the discrepancy towards estimated total sulphur deposition to downwind ecosystems were estimated relative to 2013 emissions levels, with the satellite-derived values leaving the area of regional critical load exceedances of aquatic ecosystems largely unchanged from 2013 values, 335,000 km^2, and reported values potentially decreasing this area to 185,000 km^2.

Introduction

Space-based sensors have been widely used to derive or constrain emissions of air pollutants since the mid-1990s (e.g., Streets *et al.*, 2013). Most of these early "top-down" efforts involved a form of inverse modelling in which emissions are derived such that simulation of the satellite observations from an atmospheric model agree with the satellite observations. More recently, direct approaches have been developed, in which the satellite observations are paired with winds from a meteorological reanalysis (Beirle *et al.*, 2011; Fioletov et al., 2015). This newer approach is best suited for short(er)-lived species, but it has also proved useful for intermediate (CO; Pommier *et al.*, 2013) and long-lived (CO_2; Nassar *et al.*, 2017) pollutants.

One successful application of this direct approach has been in deriving emissions of sulfur dioxide (SO_2) from the Ozone Monitoring Instrument (OMI; Levelt *et al.*, 2005; 2018; Krotkov *et al.*, 2016). A global catalogue consisting of roughly 500 sources and

their annual emissions was compiled using this methodology (Fioletov *et al.*, 2016b; NASA, 2019), is updated annually and includes sources not captured in bottom-up inventories (McLinden *et al.*, 2016), and recently was merged with a leading bottom-up gridded inventory (Liu *et al.*, 2018). The ability of OMI to capture annually varying emissions has been demonstrated for many sources globally, including power plants (Fioletov *et al.*, 2016b), smelters (Iolongo *et al.*, 2018), and volcanos (McLinden *et al.*, 2016).

This methodology was applied to the Athabasca Oil Sands Region (AOSR) in the Canadian province of Alberta, and in particular the surface mining region in the northwest corner of the AOSR (roughly 57ºN, 111ºW; just north of the community of Fort McMurray). Large deposits of bitumen (a viscous form of oil) reside within the AOSR. Extraction of bitumen, and its subsequent upgrading to a synthetic crude oil, has increased rapidly in recent years. In 2018, production from the AOSR was (the equivalent of) 3.0 million barrels of oil per day (mBPD) from bitumen, a number expected to rise to 4.2 mBPD by 2028 (AER, 2019). The process of upgrading can lead to the release of large amounts of SO_2 (McLinden *et al.*, 2012; 2016), and other pollutants (Li *et al.*, 2018; Gordon *et al.*, 2015). According to the bottom-up reported emissions of the Canadian National Pollutant Release Inventory (NPRI), the surface mining region emitted 90-100 kt[SO_2]/yr (hereafter kt/yr will be used) prior to 2013, but less than half of that in subsequent years due to the installation of control devices. In contrast, and as will be elucidated below, our evaluation using OMI observations finds emissions similar before and after installation of the devices, in broad agreement with measurements of surface concentrations in the vicinity of the emissions sources.

In this work, SO_2 data from multiple sources – emissions monitoring, surface *in-situ*, surface remote sensing, and satellites – are brought together in an attempt to understand this discrepancy. Previous work (Makar *et al.*, 2018) found exceedances of critical loads associated with AOSR emissions were occurring over a region greater than 320,000 km^2: the extent to which subsequent emissions levels have been reduced thus has a critical impact on potential long-term environmental damage in the region. Here, a critical load is a quantitative estimate of an exposure to one or more pollutants below which significant harmful effects on specified sensitive elements of the environment do

not occur (Nilsson and Grennfelt, 1988). Estimates of the potential impacts of the top-down versus bottom-up emissions estimates are provided as part of the analysis.

Datasets and methods

Oil Sands Emissions data

Reported SO_2 emissions in the oil sands include hourly emissions measured by continuous emissions monitoring systems (CEMS) on the main stacks (AG, 1998), which emit most of the SO_2 at upgrading facilities, as well as engineering estimates for emissions from other sources SO_2, such as flaring. Facility-level emissions data were retrieved from the Canadian National Pollutant Release Inventory (NPRI, 2019). Further, monthly and hourly emissions estimates and related quantities from CEMS and industrial monitoring reports, which include CEMS, flaring estimates and other SO_2 emission sources, were also used (AG, 2016). The emissions data in the NPRI and the industrial monitoring reports are generated using similar datasets and methodologies and are therefore consistent.

Figure 1 shows an image of the oil sands surface mining region. There are smaller amounts of SO_2 emitted from mobile sources, but the vast majority of emissions come from three upgraders with the two largest responsible for more than 90% of total emissions in the area over this 2005-2018 period. These are Syncrude-Mildred Lake (referred to here as SML; NPRI ID 2274; main stack height is 183 m) and Suncor (SUN, NPRI ID 2230; main stack height is 137 m), shown in Figure 1, and emit in roughly a 3:1 (SML:SUN) ratio. The height of secondary and flaring stacks, and those at the smaller CNRL upgrader, are in the range of 50-110 m. In the mid-2000s SML undertook the Sulphur Emission Reduction Plan (SERP), an initiative to retrofit flue gas desulfurization facilities, or "scrubbers", into the operation of Syncrude's two original cokers. Completed and brought online in late 2013, SML reported emissions fell from 73 kt/yr in 2012 to 28 kt by 2014. A decline at SUN was also reported, 22 to 13 kt/yr, between 2010-2015 which is attributed to a series of improvement initiatives and plant

optimizations. Since 2009 or so, the total amount of bitumen mined at SUN and SML, a good proxy for bitumen upgraded, has remained roughly constant (AER, 2020).

In-situ monitoring

The Wood Buffalo Environmental Association (WBEA, 2019) monitors the environment of the Regional Municipality of Wood Buffalo in north-eastern Alberta, including robust passive and continuous surface monitoring networks in and around the surface mines (Percy, 2013; Bari and Kindzierski, 2015; Hsu, 2013). Identified in Figure 1, there are a dozen stations within a 50 km radius of the SML/SUN upgraders outfitted with continuous Thermo Scientific 43i SO_2 analyzers (sampling height of 4 m), including four stations within 10 km (Lower Camp, Mildred Lake, Buffalo Viewpoint, and Mannix). The peak levels of SO_2 (annual 99th percentile of hourly averages) increased sharply in 2014, primarily at Lower Camp, prompting the government of Alberta to study the issue (AEP, 2018).

WBEA also operates a network of Maxxam Analytics passive SO_2 monitors (sampling height are variable, see SM; Tang, 2001), which are deployed for approximately 1-2 months during which air pollutants are adsorbed onto a filter. The ambient concentration of SO_2 is calculated from the mass of SO_2 on the filter, analyzed in a laboratory, and an estimated rate of uptake. Annual average SO_2 from passive samplers was compared against continuous analyzers across Alberta and are in good agreement, as discussed in the Supplemental Material (SM).

Satellite observations and Emissions

Satellite remote sensing can be used to derive SO_2 abundances by measuring the intensity of back-scattered Sunlight in the ultraviolet where SO_2 absorbs. The two nadir-viewing (down-looking) spectrometers used in this work are OMI on the Aura satellite (2004-present; Levelt *et al.*, 2006; 2018) and the Tropospheric Monitoring Instrument (TROPOMI) on-board the Sentinel-5 precursor (2017-present; Veefkind *et al.*, 2012). Retrievals are performed by first matching laboratory-measured SO_2 absorption cross-sections and other relevant parameters to these observed spectra which provide a

determination of the SO_2 slant column densities (SCDs), or the SO_2 number density integrated along the path of the sunlight through the atmosphere. SCDs were then converted to the more physically-meaningful vertical column density (VCD), the vertically-integrated SO_2 number density, using an air mass factor (AMF) which quantifies the sensitivity of the satellite to a particular scene. In practical terms, a multiple-scattering model is used to calculate AMFs (Palmer *et al.*, 2001) which depends on factors such as solar and viewing geometry, the presence of clouds, scene reflectivity and the vertical distribution of the SO_2. VCDs are then determined through VCD=SCD/AMF.

OMI observations date back to late 2004, and hence are extremely useful to track the temporal evolution of SO_2 and its emissions. With a spatial resolution of 13×24 km^2 at best, and more typically 15×35 km^2 – distances that are comparable to the entirety of the surface mining region – data spanning multiple years are analyzed together. The OMI SO_2 product used here is version 3.1, which utilizes the Principle-Component Analysis (PCA) retrieval algorithm developed by Li *et al.* (2013). The standard NASA OMI SO_2 product uses a spatial and temporally invariant AMF, calculated for summertime conditions in the eastern US (AMF=0.36; Li *et al.*, 2013). TROPOMI, the successor to OMI, has a much shorter data record (effectively March 2018 to present) but with its much higher spatial resolution (3.5×7 km^2) it can better capture details of the spatial distribution. The official European Space Agency TROPOMI SO_2 data product is used here (RPRO version 010105) (Theys *et al.*, 2017) and is calculated using scene-specific AMFs based on input information at a spatial resolution of 1.0°.

To improve the effective spatial resolution, OMI and TROPOMI AMFs were reprocessed using higher resolution input information (McLinden et al., 2014) as discussed further in the SM. Also, our analysis was limited to observations between April and October where Sun angles are high (see Figure S4). A further examination of this approximation and details on data screening are given in the SM.

Satellite observations were also used to derive emissions using methods developed for point-sources (Fioletov *et al.*, 2015) and multiple or area sources (Fioletov et al., 2017). As is expanded upon in the SM, these methods are based on the observed VCDs combined with coincident winds from a meteorological reanalysis. Emissions

were obtained by fitting the satellite observations and winds to an Exponentially Modified Gaussian (EMG) plume function (Fioletov *et al.*, 2015) based on an effective lifetime, derived as part of the analysis, of 4.0 hours. Multiple years of observations and winds are analyzed together in order to reduce noise. Further details on the emissions calculations and a detailed error budget are provided in the SM.

Pandora Spectrometer

In addition to the traditional *in-situ* ground-based SO_2 instruments, a Pandora spectrometer has been operating at the Oski-Otin (see Figure 1) monitoring site in Fort McKay since August 2013 (with intermittent gaps) (Fioletov *et al.*, 2016a). Pandora is a remote sensing instrument that measures direct UV-visible sunlight transmitted through the atmosphere in the ultraviolet (Herman *et al.*, 2009). Unlike the satellite-sensors, conversion of direct-Sun SCD to VCD is straightforward and based purely on geometry, making it a more accurate method. One clear advantage of observing VCD as opposed to surface concentrations is that it is sensitive to plumes aloft.

Here observations from Pandora #104 (Aug-Oct 2013; Oct 2014-Feb 2016) and #122 (Sept 2017-Dec 2018, except May 2018) were considered. While #122 replaced #104, the monthly-calibration procedure (Fioletov et al., 2016a) ensures there are no appreciable inter-instrument offsets and no distinction will be made between the two instruments in our interpretation. It is noted that the Pandora monitors are located to the N/NW of the SML/SUN upgraders, and that winds at the Pandora site originate from that direction during 15-20% of the data record.

Results

Figure 2 shows reported annual SO_2 emissions from the AOSR surface mining area, total and flaring. In the second half of 2013, additional scrubbers came online at SML with the impact of these scrubbers being the inferred cause for the reported factor of three decrease beginning in 2014, and a factor of two decrease in overall emissions from the upgraders. However, this decrease in reported emissions is not matched by a decrease in ambient SO_2 levels. Figure 2 also shows the time series of annual mean SO_2 from several

continuous WBEA surface stations in the area with the multi-station averages indicating a slow decline between 2002 and 2013, broadly consistent with emissions. Subsequent to this, however, there is an increase of 20-30%, peaking in 2016, before a subsequent decrease back to 2013-2014 levels. These surface concentration trends are followed whether one considers the four continuous stations in the immediate vicinity of the upgraders (<10 km) or all continuous stations throughout the surface mining area. Nearby WBEA passive SO_2 sensors are broadly consistent with the continuous monitoring although their post-2013 increase is less pronounced.

In an effort to understand this apparent discrepancy, which was also noted by Edgerton et al. (2019), satellite remote sensing was utilized as it provides an integrated view of the area. Previous analyses of OMI SO_2 revealed elevated VCDs (or "hot-spots") within 30-40 km of the upgraders (McLinden *et al.*, 2012; 2016) although these studies only considered observations up to 2014. An updated analysis is presented here: average (April-October) OMI SO_2 VCD are shown in Figure 3 for two four-year periods: 2010-2013 and 2014-2017, which roughly coincide to the pre- and post- drop in reported emissions. A more detailed view is provided in the Figure S0 which shows running 3-year means, spanning 2005-2007 to 2017-2019. Consistent with the previous studies, Figure 3 shows a maximum near the two large upgrading sources, SML and SUN. Most importantly, it also shows a modest increase in SO_2 for 2014-2017, relative to 2010-2013.

Also shown in Figure 3 are maps derived from the WBEA station observations. Multi-annual (2010-2013 and 2014-2017) mean SO_2 from the passive and continuous stations were taken together and then averaged onto the same 2 × 2 km grid using an inverse distance-squared weighting. When both continuous and passive observations were made at the same station, their mean was used, and only grid-boxes where 3 or more stations were within 30 km were retained. These interpolated maps show the same general characteristics as the OMI maps, including a hot spot around the SML and SUN upgraders, as well as a slight increase in the latter period.

In addition to mapping spatial distributions, OMI observations were used to derive emissions, thereby enabling a quantitative comparison with reported emissions. Running three-year emissions time series from OMI are compared with the reported emissions in Figure 4a. The three different OMI emissions algorithm variants, as mentioned above described in more detail in the SM, were used. These are (i) assuming a single point source located between SUN and SML, (ii) a multi-source approach assuming emissions from the three (SML, SUN, CNRL) upgrader locations, and (iii) a multi-source approach allowing for a 3×3 grid of potential emission locations which does not assume the location of emissions but lets the algorithm determine where to place them to best match observations. These three variants produce emissions that are all quite consistent with each other, and with the two multi-source approaches, (ii) and (iii), well within the point-source uncertainty estimate, for which a detailed error budget was developed (See Table S2). It is worth noting here that OMI has demonstrated its ability to track changes in SO_2 emissions at other locations (e.g., Fioletov *et al.*, 2016; Iolongo *et al.*, 2018). Two specific examples at a latitude comparable to the oil sands, shown in Figure S3, are a copper smelter in Flin Flon, Manitoba, Canada, in which OMI captures the rapid decrease resulting from its decommissioning, and a nickel smelter in Thompson, Manitoba where both OMI and NPRI indicate an approximate 5%/year decline.

From Figure 4a, up until 2013, OMI compares well with the reported emissions which suggests there are no significant systematic errors in the OMI emissions. This is important as the largest potential source of uncertainty in OMI emissions are systematic, and manifest as a relative error that is largely time independent. The decrease in reported emissions beginning in 2014 is not apparent in the OMI-estimated emissions. Rather, OMI emissions estimates show a similar trend to WBEA monitoring of ambient SO_2; flat, or increasing, then decreasing in the last 1-2 years. An estimate of the additional SO_2 emissions required to reconcile this difference was obtained simply by subtracting the reported emissions from those estimated from OMI. Near zero for the first several years, the magnitude of this difference reaches 50 kt/yr in 2016. To place this into context, the discrepancy's magnitude is similar to that of some of the largest emissions sources in Canada with only two other operations Canada-wide reporting SO_2 emissions in excess of

30 kt/yr for 2017 (NPRI, 2019). Figure 4b is a synthesis of Figures 2 and 4a, better demonstrating the contrast between the various sources of SO_2 information (reported emissions, OMI emissions, and surface monitoring) by showing relative changes. Figure 4b further highlights the gap between reported emissions and the observation-based quantities. However, by 2017-2018, OMI does suggest a decrease in emissions of about 30% relative to pre-2014 values, which bridges much of the gap with the reported emissions. By contrast, the surface monitoring continues to show no significant decrease relative to pre-2014. The cause for the better agreement between OMI and reported emissions remains unclear.

There is one additional source of multi-year SO_2 observations from the area: Pandora spectrometer observations from the Oski-Otin monitoring site in Fort McKay, roughly 20 km N/NW of the upgraders (see Figure 1). When analyzed as a function of wind direction, as in Figure S7, there is a clear peak in VCD only for winds originating from the general direction of the SML and SUN upgraders (Fioletov *et al.*, 2016a). The two periods of Pandora data are late-2013 to 2015 (referred to as P1), and late-2017-2018 (P2), each with multiple months where the instrument was not operating. Considering only observations with the wind from the SML/SUN upgraders (130-190°), average Pandora VCD dropped by 23±14% between P1 and P2. This might appear as evidence of the expected drop in emissions from the scrubbers except that (i) for the large majority (if not all) of P1 the scrubbers were on-line and (ii) this appears to be sampling artifact based on the specific months the Pandora was operating for each period. Considering only the months of Pandora operation, the average monthly reported emissions were virtually unchanged between P1 and P2. By contrast, the average amount of bitumen produced at SML and SUN – generally an excellent proxy for emissions – dropped by 16% from P1 to P2, making it consistent with Pandora within uncertainties. Sampling the four continuous WBEA stations nearest the upgraders in the same way, there is a 19% decrease between P1 and P2. When annual totals or averages are considered, bitumen production was flat while the four continuous WBEA stations showed an increase (see, e.g., Figure 2) from P1 to P2, substantiating the claim that Pandora sampling was an issue. All told, Pandora is able to corroborate that significant emissions originate only

from the SML/SUN direction and is consistent with the other SO_2 observations, but given a lack of observations from the pre-scrubber period, it cannot specifically address the question of how emissions changed as a result.

While OMI is ideal to track the evolution of SO_2 due to its long data record, the TROPOMI satellite sensor, owing to its superior spatial resolution, is much better suited to help isolate the location of the current emissions. Figure 5 shows the TROPOMI 2018 (April-Oct.) average SO_2. Here SCDs are first presented as converting SCD to VCD requires an assumption about the location of the sources. Thus, SCD is preferred when there may be some uncertainty as to the source location(s). To better delineate the location of origin, averages were calculated considering only wind speeds (between 950-900 hPa) below the median value to limit how far the emitted SO_2 can travel before chemical transformation or deposition. The distribution of TROPOMI VCD, shown in Figure 5b, is very similar to SCD. This combination of higher resolution and low winds indicates the location of all significant sources of SO_2 to be isolated to the immediate vicinity of the Syncrude and Suncor upgraders, or somewhere in between, within roughly a 10×10 km^2 box, as shown in Figure 5c. This source area is completely consistent with the sector identified by the Pandora, also shown in Figure 5c.

Discussion

The atmospheric observations considered here, collectively, suggest that total SO_2 emissions in the surface mining region did not decline in 2014 as suggested by the emission reports, although there is mixed evidence that a more modest decline occurred around 2018. They also confirm that any sources of SO_2 are limited to a small region in the immediate vicinity of the SUN or SML upgraders. While, at present, no satisfactory explanation exists that reconciles the reported and top-down emissions, it is nonetheless worthwhile exploring the potential explanations.

One possible reason, differences in meteorological conditions, can be ruled out immediately as distributions of wind speeds and direction show no significant differences

for the 2010-2013 and 2014-2017 periods. This is true when examining the meteorological reanalyses and the WBEA station data (see Figure S5). The efficacy of the scrubbers is considered next. The majority, roughly 80-90% (see Figure 2), of the reported SML and SUN SO_2 emissions are from the stacks in which SO_2 has been scrubbed and monitored using CEMS, a direct and reliable measurement of stack emissions. According to monthly emission reports (AG, 2016), the remaining SO_2 is emitted from flaring stacks in which the high temperature of emissions prevents the use of CEMS, and emissions estimates for these sources are consequently based on engineering estimates rather than direct observation, and have a higher degree of uncertainty. Since the SML CEMS indicates an approximate three-fold decrease in emissions, the scrubbers appear to be operating as expected, reducing SO_2 reaching the main, non-flaring stacks.

This decrease and the broad consistency between atmospheric observations and reported emissions up until 2014 suggests that any explanation must include some kind of transition towards higher emissions from non-CEMS sources in 2013-2014. One possibility is that a completely new source emerged around this time, with a magnitude sufficient to cancel whatever reductions were gained from the scrubbers. For example, tailings ponds are known to emit a mixture of air pollutants (Galarneau *et al.*, 2014), as do the surface mines themselves (Liggio *et al.*, 2016). However, this possibility seems unlikely given the required magnitude of the source, 10's of kt/yr, and the need for an explanation for its absence prior to 2014 given similar types of activities in the mines before and after that time. Another non-CEMS source is flaring. This source cannot, at present, be discounted but yet there is no clear evidence pointing to this possibility.

It is reiterated that (i) both the surface and satellite SO_2 observations employed here agree in their trends before and after 2014 and (ii) the CEMS monitors are reporting the SO_2 concentrations with significant reductions from upstream emissions. It is further assumed that (iii) no new significant sources of SO_2 emerged in 2013-2014 and (iv) that the process of upgrading contributes most of the facilities' SO_2 emissions (as evidenced by the regulatory requirement of scrubbers). If these statements are all valid, they suggest

that a significant fraction of SO_2 upgrading emissions originate from a pathway not connected to the scrubbers.

Concentrations of SO_2 in the region are controlled by emissions, and hence both dry and wet total sulphur deposition. The latter are used to determine exceedances of critical loads, which are used to assess risk of potential future ecosystem damage associated with acidifying deposition (Makar et al, 2018). A difference of 60% in emissions levels has a significant impact on the size of the region at risk of future ecosystem damage, as we demonstrate here. Previous work (Makar *et al*., 2018) combined observation-corrected modelled deposition fields, and internationally established protocols for the creation of critical loads, to estimate the potential damage to downwind terrestrial and aquatic ecosystems associated with acidifying deposition. Exceedances of critical loads for aquatic ecosystems (a measure of the potential for eventual aquatic ecosystem damage, if emissions continue at a given level) were predicted for a large region (334,000 km^2 for aquatic ecosystems; approximately half of the size of the provinces of Alberta or Saskatchewan; see Figure 6a). However, the study made use of 2013 emissions data, i.e., just prior to the large decrease in the reported SO_2 emissions. Using this combination of observation-corrected model output and critical loads, an estimate of the size of the area in exceedance resulting from a 40% reduction in emissions (the percent reduction between 2013 and 2016 in the reported emissions data) is shown in Figure 6b. The latter is an approximation with the assumptions that SO_2 surface concentrations (and hence SO_2 deposition fluxes) will be linearly proportional to SO_2 emissions levels, and that all SO_2 emissions in the model domain were reduced by 40%. The area in exceedance would decrease by 44.5% relative to 2013, a substantial reduction in potential environmental impacts associated with the emissions. However, if no change in emissions has occurred (as implied by the satellite-derived emissions and the surface concentration monitoring network data), then the area in exceedance of critical loads will be the same as predicted in Figure 6a.

Finally, we note that recent work examining sulphur uptake to multiple forms of vegetation in the oil sands region on a yearly basis between 2009 and 2016 is in accord

with our results (Wieder et al, 2020). In that work, no decrease in sulphur uptake was observed between the years 2014 to 2016, despite the factor of two decrease in reported SO_2 emissions. We thus have three independent sources of information (satellite observations, surface concentration observation, and sulphur uptake in vegetation) which show no evidence of a decrease in SO_2 loading within the 2014 to 2016 time period.

Acknowledgements

We acknowledge the helpful comments from two anonymous reviewers. We also acknowledge the NASA Earth Science Division for funding of OMI SO_2 products development and analysis. This work was partially funded under the Oil Sands Monitoring Program and is a contribution to the Program but does not necessarily reflect the position of the Program.

Data Availability

WBEA continuous station data are available from https://wbea.org/historical-monitoring-data/ and data from the passive stations from https://wbea.org/resources/reports-publications/air-monitoring-reports/integrated-samples-lab-results/. The OMI level 2 SO_2 data product is available from the NASA Earth Observing System Data and Information System (https://aura.gesdisc.eosdis.nasa.gov/data/Aura_OMI_Level2/OMSO2.003/). The TROPOMI level 2 SO_2 data are available from Sentinel-5p Pre-Operations data hub (https://s5phub.copernicus.eu/dhus/#/home). Reanalyses can be downloaded from the ECMWF portal (https://apps.ecmwf.int/datasets/). NPRI annual emissions data can be obtained from https://www.canada.ca/en/services/environment/pollution-waste-management/national-pollutant-release-inventory.html. The re-processed level 2 OMI and TROPOMI data, with the ECCC air mass factors, and the Pandora SO_2 data can be downloaded from http://collaboration.cmc.ec.gc.ca/cmc/arqi/OilSands_Satellite_SO2datasets/.

References

Alberta Environment and Parks (AEP), Lower Athabasca Region Status of Management Response for Environmental Management Framework, as of October 2017. Government of Alberta. ISBN 978-1-4601-3198-5. Available at https://open.alberta.ca/publications/9781460136799, 2018.

AER (Alberta Energy Regulator) (2019), ST98-2019: Alberta Energy Outlook. Available at https://www.aer.ca/providing-information/data-and-reports/statistical-reports/st98

AER (Alberta Energy Regulator) (2020), ST39: Alberta Mineable Oil Sands Plant Statistics Monthly Supplement. Available at https://www.aer.ca/providing-information/data-and-reports/statistical-reports/st39.html

Alberta Government (AG), Continuous Emission Monitoring System (CEMS) Code, 1998, ISBN 0-7732-5038-7. Available at https://open.alberta.ca/publications/0773250387, 1998.

Alberta Government (AG), Air Monitoring Directive Chapter 9: Reporting, AEP, Air Policy, 2016, No. 1-9. ISBN 978-1-4601-3198-5. Available at https://open.alberta.ca/dataset/9f75b54e-641a-4d9d-885f-e87e973321b4/resource/97ffd485-2bd3-44e8-a691-b115cb368913/download/amd-chapter9-reporting-dec16-2016a.pdf, 2016

Bari, M. and W.B. Kindzierski, Fifteen-year trends in criteria air pollutants in oil sands communities of Alberta, Canada, Environment International 74 (2015) 200–208 201, DOI: 10.1016/j.envint.2014.10.009

Beirle, S., Boersma, K. F., Platt, U., Lawrence, M. G., and Wagner, T.: Megacity Emissions and Lifetimes of Nitrogen Oxides Probed from Space, Science, 333, 1737-1739, 2011.

Dee, D. P., Uppala, S. M., Simmons, A. J., Berrisford, P., Poli, P., Kobayashi, S., Andrae, U., Balmaseda, M. A., Balsamo, G., Bauer, P., Bechtold, P., Beljaars, A. C. M., van de Berg, L., Bidlot, J., Bormann, N., Delsol, C., Dragani, R., Fuentes, M., Geer, A. J., Haimberger, L., Healy, S. B., Hersbach, H., Hólm, E. V., Isaksen, L., Kållberg, P., Köhler, M., Matricardi, M., McNally, A. P., Monge-Sanz, B. M., Morcrette, J.-J., Park, B.-K., Peubey, C., de Rosnay, P., Tavolato, C., Thépaut, J.-

N. and Vitart, F. (2011), The ERA-Interim reanalysis: configuration and performance of the data assimilation system. Q.J.R. Meteorol. Soc., 137: 553–597. doi: 10.1002/qj.828

Edgerton, E. S, Y-M. Hsu, E.M. White, M.S. Landis, M.E. Fenn, Ambient Concentrations and Total Deposition of Inorganic Sulfur, Inorganic Nitrogen and Base Cations in the Athabasca Oil Sands Region, Sci. Total Env., doi: https://doi.org/10.1016/j.scitotenv.2019.134864, 2019.

Fioletov, V. E., C. A. McLinden, N Krotkov, M. D. Moran, and K. Yang, Estimation of SO_2 emissions using OMI retrievals, Geophys. Res. Lett., 38, L21811, doi:10.1029/2011GL049402, 2011.

Fioletov, V. E., C. A. McLinden, N. Krotkov, and C. Li (2015), Lifetimes and emissions of SO_2 from point sources estimated from OMI, *Geophys. Res. Lett.,* 42, https://doi.org/10.1002/2015GL063148, 2015.

Fioletov, V. E., C. A. McLinden, A. Cede, J. Davies, C. Mihele, S. Netcheva, S.-M. Li, and J. O'Brien, Sulphur dioxide (SO2) vertical column density measurements by Pandora spectrometer over the Canadian oil sands, Atmos. Meas. Tech, 9, 2961–2976, doi:10.5194/amt-9-2961-2016, 2016a.

Fioletov, V. E., C. A. McLinden, N. Krotkov, C. Li, J. Joiner, N. Theys, and M. D. Moran, A global catalogue of large SO_2 sources and emissions derived from the Ozone Monitoring Instrument, Atmos. Chem. Phys., 16, 11497–11519, doi:10.5194/acp-16-11497-2016, 2016b.

Fioletov, V., C. A. McLinden, S. K. Kharol, N. A. Krotkov, C. Li, J. Joiner, M. D. Moran, R. Vet, A. J. H. Visschedijk, and H. A. C. Denier van der Gon, Multi-source SO2 emissions retrievals and consistency of satellite and surface measurements with reported emissions, Atmos. Chem. Phys., 17, doi:10.5194/acp-2017-485, 2017.

Galarneau, E., B. P. Hollebone, Z. Yang, and J. Schuster, Preliminary measurement-based estimates of PAH emissions from oil sands tailings ponds, Atmos. Env., 97, 332-335, 2014.

Gordon, M., Li, S.-M., Staebler, R., Darlington, A., Hayden, K., O'Brien, J., and Wolde, M.: Determining air pollutant emission rates based on mass balance using

airborne measurement data over the Alberta oil sands operations, Atmos. Meas. Tech., 8, 3745–3765, https://doi.org/10.5194/amt-8-3745-2015, 2015..

Griffin, D., X. Zhao, C. A. McLinden, F. Boersma, A. Bourassa, E. Dammers, D. Degenstein, H. Eskes, L. Fehr, V. Fioletov, K. Hayden, S. K. Kharol, S.-M. Li, P. Makar, R. V. Martin, C. Mihele, R. L. Mittermeier, N. Krotkov, M. Sneep, L. N. Lamsal, M. ter Linden, J. van Geffen, P. Veefkind, and M. Wolde, High resolution mapping of nitrogen dioxide with TROPOMI: First results and validation over the Canadian oil sands, Geophys. Res. Lett., 45, https://doi.org/10.1029/2018GL081095, 2018.

Helfrich, S. R., McNamara, D., Ramsay, B. H., Baldwin, T., and Kasheta, T.: Enhancements to, and forthcoming developments in the Interactive Multisensor Snow and Ice Mapping System (IMS). Hydrological Processes, 21, 1576−1586. doi:10.1002/HYP.6720, 2007.

Herman, J., Cede, A., Spinei, E., Mount, G., Tzortziou, M. and Abuhassan, N.: NO2 column amounts from ground-based Pandora and MFDOAS spectrometers using the direct-sun DOAS technique: Intercomparisons and application to OMI validation, J. Geophys. Res., 114(D13), D13307, doi:10.1029/2009JD011848, 2009.

Ialongo, I., V. Fioletov, C. McLinden, M. Jåfs, N. Krotkov, C. Li, and J. Tamminen, Application of satellite-based sulfur dioxide observations to support the cleantech sector: Detecting emission reduction from copper smelters, Env. Tech. Inn., 12, 172–179, 2018

Kelly, E. N., *et al.*, Oil sands development contributes elements toxic at low concentrations to the Athabasca River and its tributaries, Proc. Nat. Academy Sci., 107, 16178–16183, 2010.

Krotkov, N. A., C. A. McLinden, C. Li,1, L. N. Lamsal, E. A. Celarier, S. V. Marchenko, W. H. Swartz, E. J. Bucsela, J. Joiner, B. N. Duncan, K. F. Boersma, J. P. Veefkind, P. F. Levelt, V. E. Fioletov, R. R. Dickerson, H. He, Z. Lu, and D. G. Streets, Aura OMI observations of regional SO2 and NO2 pollution changes from 2005 to 2015, Atmos. Chem. Phys., 16, 4605–4629, doi:10.5194/acp-16-4605-2016.

Levelt, P., Joiner, J., Tamminen, J., Veefkind, J. P., Bhartia, P. K., Stein Zweers, D. C., Duncan, B. N., Streets, D. G., Eskes, H., van der A, R., McLinden, C., Fioletov, V., Carn, S., de Laat, J., DeLand, M., Marchenko, S., McPeters, R., Ziemke, J., Fu, D., Liu, X., Pickering, K., Apituley, A., González Abad, G., Arola, A., Boersma, F., Chan Miller, C., Chance, K., de Graaf, M., Hakkarainen, J., Hassinen, S., Ialongo, I., Kleipool, Q., Krotkov, N., Li, C., Lamsal, L., Newman, P., Nowlan, C., Suleiman, R., Tilstra, L. G., Torres, O., Wang, H., and Wargan, K.., The Ozone Monitoring Instrument: overview of 14 years in space, Atmos. Chem. Phys., 18, 5699-5745, https://doi.org/10.5194/acp-18-5699-2018, 2018.

Levelt, P. F., van den Oord, G. H. J., Dobber, M. R., Mälkki, A., Visser, H., de Vries, J., Stammes, P., Lundell, J. O. V., and Saari, H.: The Ozone Monitoring Instrument, *IEEE Trans. Geosci. Remote Sens.*, 44, 1093-1101, 2006.

Li, C., J. Joiner, N. A. Krotkov, and P. K. Bhartia (2013), A fast and sensitive new satellite SO2 retrieval algorithm based on principal component analysis: Application to the ozone monitoring instrument, Geophys. Res. Lett., 40, 6314–6318, doi:10.1002/2013GL058134.

Li, S.-M., Amy Leithead, Samar G. Moussa, John Liggio, Michael D. Moran, Daniel Wang, Katherine Hayden, Andrea Darlington, Mark Gordon, Ralf Staebler, Paul A. Makar, Craig A. Stroud, Robert McLaren, Peter S. K. Liu, Jason O'Brien, Richard L. Mittermeier, Junhua Zhang, George Marson, Stewart G. Cober, Mengistu Wolde, Jeremy J. B. Wentzell, Differences between measured and reported volatile organic compound emissions from oil sands facilities in Alberta, Canada, Proceedings of the National Academy of Sciences Apr 2017, 201617862; DOI: 10.1073/pnas.1617862114

Liggio J, *et al.*, Oil sands operations as a large source of secondary organic aerosols. Nature 534:91–94, 2016.

Liggio, J., Li, S.-M., Staebler, R., Hayden, K., Darlington, A., Mittermeier, R., O'Brien, J., McLaren, R., Wolde, M., Worthy, D., andVogel, F.: Measured Canadian oil sands CO_2 emissions are higher than estimates made using internationally recommended methods, Nature Communications, 10, https://doi.org/10.1038/s41467-019-09714-9, 2019

Liu, F., Choi, S., Li, C., Fioletov, V. E., McLinden, C. A., Joiner, J., Krotkov, N. A., Bian, H., Janssens-Maenhout, G., Darmenov, A. S., and da Silva, A. M.: A new global anthropogenic SO2 emission inventory for the last decade: a mosaic of satellite-derived and bottom-up emissions, Atmos. Chem. Phys., 18, 16571-16586, https://doi.org/10.5194/acp-18-16571-2018, 2018

Makar, P., Gong, w., Milbrandt, J., Hogrefe, C., Zhang, Y., Curci, G., *et al.* (2015). Feedbacks between air pollution and weather, Part 1: Effects on weather. Atmospheric Environment, 115, 442–469.

Makar, P. A., Akingunola, A., Aherne, J., Cole, A. S., Aklilu, Y.-A., Zhang, J., Wong, I., Hayden, K., Li, S.-M., Kirk, J., Scott, K., Moran, M. D., Robichaud, A., Cathcart, H., Baratzedah, P., Pabla, B., Cheung, P., Zheng, Q., and Jeffries, D. S.: Estimates of exceedances of critical loads for acidifying deposition in Alberta and Saskatchewan, Atmos. Chem. Phys., 18, 9897-9927, https://doi.org/10.5194/acp-18-9897-2018, 2018.

McLinden, C. A., V. Fioletov, K. F. Boersma, N. Krotkov, C. E. Sioris, J. P. Veefkind, and K. Yang, Air quality over the Canadian oil sands: A first assessment using satellite observations, Geophys. Res. Lett., 39, L04804, doi:10.1029/2011GL050273, 2012.

McLinden, C. A., V. Fioletov, K. F. Boersma, S. Kharol, N. Krotkov, P. A. Makar, R. V. Martin, J. P. Veefkind, and K. Yang, Satellite retrievals of NO2 and SO2 over the Canadian oil sands and comparisons with surface measurements, Atmos. Chem. Phys., 14, 3637–3656, doi:10.5194/acp-14-3637-2014, 2014.

McLinden, C. A., V. Fioletov, M. W. Shephard, N. Krotkov, C. Li, R. V. Martin, M. D. Moran, and J. Joiner, Space-based detection of missing sulfur dioxide sources of global air pollution, Nature-Geoscience, doi: 10.1038/ngeo2724, 2016.

McLinden, C. A., V. Fioletov, N. Krotkov, C. Li, K. F. Boersma, and C. Adams, A decade of change in NO2 and SO2 over the Canadian oil sands as seen from space, Env. Sci. Tech., doi:10.1021/acs.est.5b04985, 2016.

McLinden, C. A., V. Fioletov, K. F. Boersma, N. Krotkov, C. E. Sioris, J. P. Veefkind, and K. Yang, Air quality over the Canadian oil sands: A first assessment using

satellite observations, Geophys. Res. Lett., 39, L04804, doi:10.1029/2011GL050273, 2012.

National Aeronautics and Space Administration (NASA), Multi-decadal Sulfur Dioxide Climatology from Satellite Instruments, https://so2.gsfc.nasa.gov/measures.html, 2019

Nassar, R., T. G. Hill, C. A. McLinden, D. Wunch, D. B. A. Jones, and D. Crisp, Quantifying CO2 emissions from individual power plants from space, Geophys. Res. Lett., 44, 10,045–10,053. https://doi.org/10.1002/2017GL074702, 2017.

National Pollutant Release Inventory (NPRI): 2019. Sulfur oxide emissions for Canada: https://www.canada.ca/en/services/environment/pollution-waste-management/national-pollutant-release-inventory.html, last access: 17 July 2019.

Nilsson, J., and Grennfelt, P.: Critical loads for sulphur and nitrogen, Report from a workshop held at Skokloster, Sweden 19–24, March 1988, Miljorapport, 15, 1–418, 1988.

Palmer, P. I., Jacob, D. J., Chance, K., Martin, R. V., Spurr, R. J. D., Kurosu, T. P., Bey, I., Yantosca, R., Fiore, A., and Li, Q., Air mass factor formulation for spectroscopic measurements from satellites: Application to formaldehyde retrievals from the Global

Ozone Monitoring Experiment, J. Geophys. Res., 106, 14539–14550, 2001.

Percy, K. E. (2013). Geoscience of Climate and Energy 11. Ambient Air Quality and Linkage to Ecosystems in the Athabasca Oil Sands, Alberta. Geoscience Canada, 40(3), 182 - 201. https://doi.org/10.12789/geocanj.2013.40.014

Pendlebury, D., Gravel, S., Moran, M. D., and Lupu, A., Impact of chemical lateral boundary conditions in a regional air quality forecast model on surface ozone predictions during stratospheric intrusions. Atmospheric Environment, 174, 148–170. https://doi.org/10.1016/j.atmosenv.2017.10.052, 2018.

Pommier, M., C. A. McLinden, and M. Deeter (2013), Relative changes in CO emissions over megacities based on observations from space, Geophys. Res. Lett., 40, doi:10.1002/grl.50704.

Schaaf, C. B., Gao, F., Strahler, A. H., Lucht, W., Li, X., Tsang, T., Strugnell, N. C., Zhang, X., Jin, Y., Muller, J.-P., Lewis, P., Barnsley, M., Hobson, P., Disney, M.,

Roberts, G., Dunderdale, M., Doll, C., d´Entremont, R. P., Hu, B., Liang, S., Privette, J. L., and Roy, D.: First operational BRDF, albedo nadir reflectance products from MODIS, Remote Sens. Environ., 83, 135–148, 2002.

Streets, D. G. *et al.* Emissions estimation from satellite retrievals: A review of current capability. Atmos. Environ. 77, 1011–1042, (2013).

Tang, H. (2001). Introduction to Maxxam all-season passive sampling system and principles of proper use of passive samplers in the field study. The Scientific World Journal, 1, 463-474.

Theys, N., De Smedt, I., Yu, H., Danckaert, T., van Gent, J., Hörmann, C., Wagner, T., Hedelt, P., Bauer, H., Romahn, F., Pedergnana, M., Loyola, D., and Van Roozendael, M.: Sulfur dioxide retrievals from TROPOMI onboard Sentinel-5 Precursor: algorithm theoretical basis, Atmos. Meas. Tech., 10, 119-153, https://doi.org/10.5194/amt-10-119-2017, 2017.

Veefkind, J. P., Aben, I., McMullan, K., Förster, H., de Vries, J., Otter, G., Claas, J., Eskes, H. J., de Haan, J. F., Kleipool, Q., van Weele, M., Hasekamp, O., Hoogeveen, R., Landgraf, J., Snel, R., Tol, P., Ingmann, P., Voors, R., Kruizinga, B., Vink, R., Visser, H., and Levelt, P. F.: TROPOMI on the ESA Sentinel-5 Precursor: A GMES mission for global observations of the atmospheric composition for climate, air quality and ozone layer applications, Remote. Sens. Environ., 120, 70–83, doi:10.1016/j.rse.2011.09.027, 2012.

Weider, R. K., M. A. Vile, K. D. Scott, C. M. Albright, J. C. Quinn, and D. H. Vitt, Bog plant/lichen tissue nitrogen and sulfur concentrations and porewater chemistry as indicators of emissions from oil sands development in Alberta, Canada, submitted, 2020.

Wood Buffalo Environment Association, https://wbea.org/, 2019.

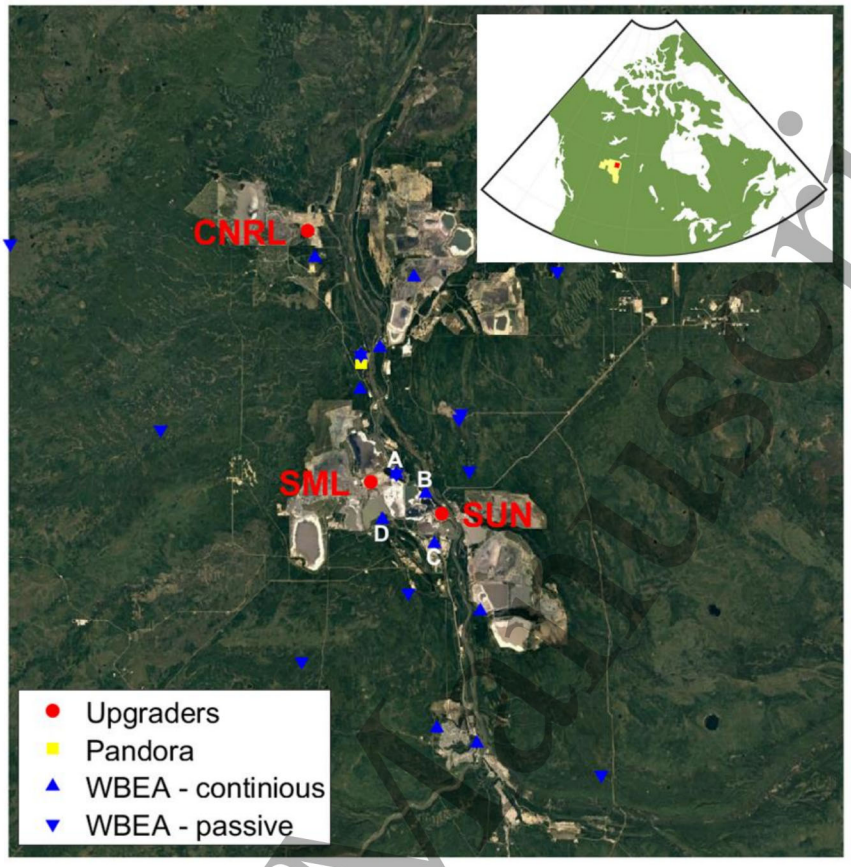

Figure 1: The surface mining domain of the AOSR. Shown are the locations of the bitumen upgraders, the only known significant source of SO_2 in the region (SUN=Suncor, SML=Syncrude-Mildred Lake, and CNRL=Canadian Natural Resources Limited, with SUN+SML contributing over 90% of the emissions), the Pandora spectrometer located at the Oski-Otin monitoring station, and the continuous and passive WBEA *in-situ* SO_2 monitors. The letters denote the WBEA monitoring stations nearest the SML and SUN upgraders (A is Mildred Lake, B is Lower Camp, C is Mannix, and D is Buffalo Viewpoint). Inset: Canada-wide map showing the AOSR (yellow) and the domain of the main map shown here (red).

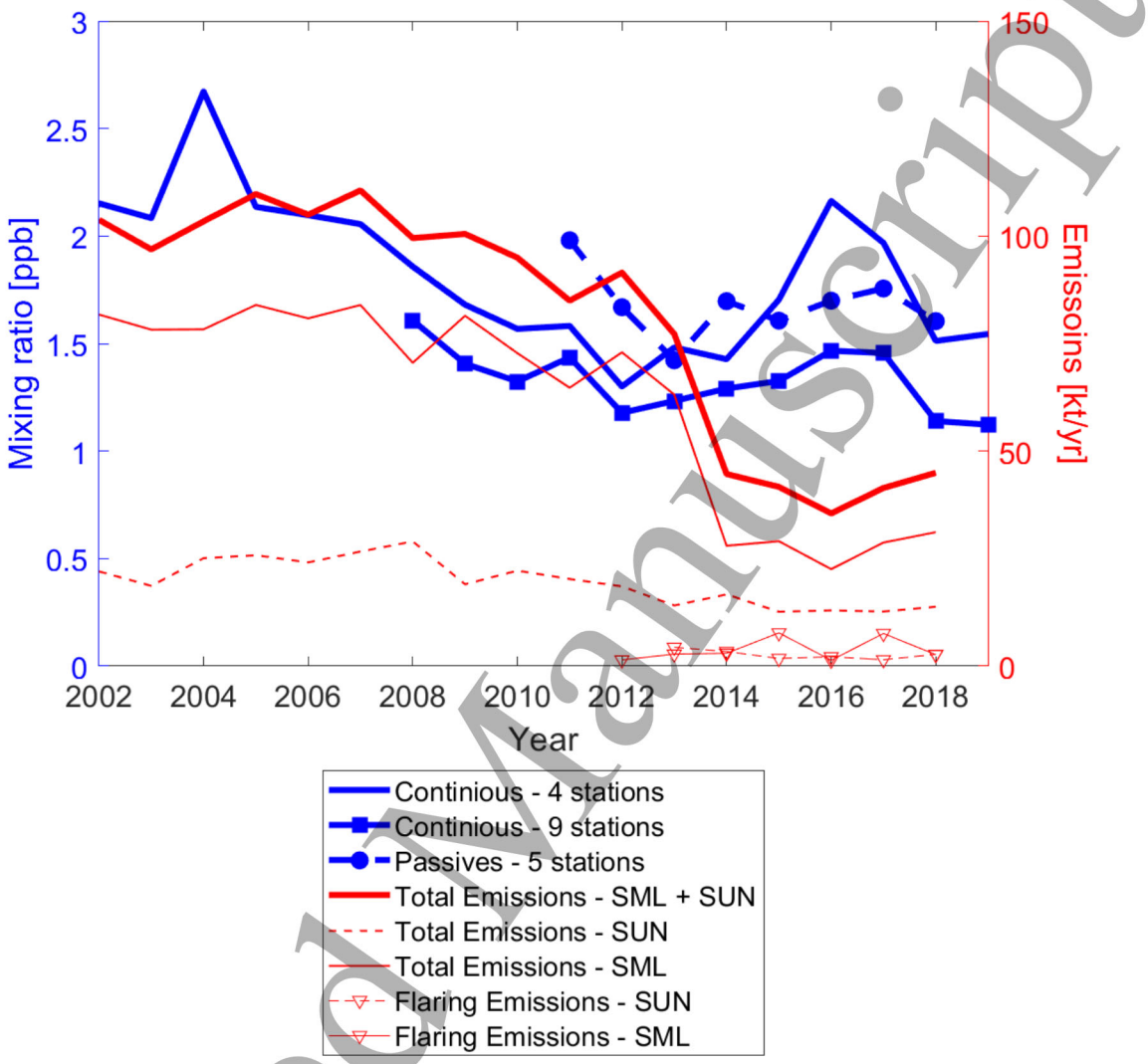

Figure 2: Time series of annual mean SO_2 averaged over different groupings of WBEA continuous and passive stations, including the four continuous stations within 10 km if the SML and SUN upgraders (Mildred Lake, Lower Camp, Buffalo Viewpoint, Mannix). Also shown (right axis) are the SO_2 emissions reported to NPRI for the SML and SUN upgraders and their flaring emissions.

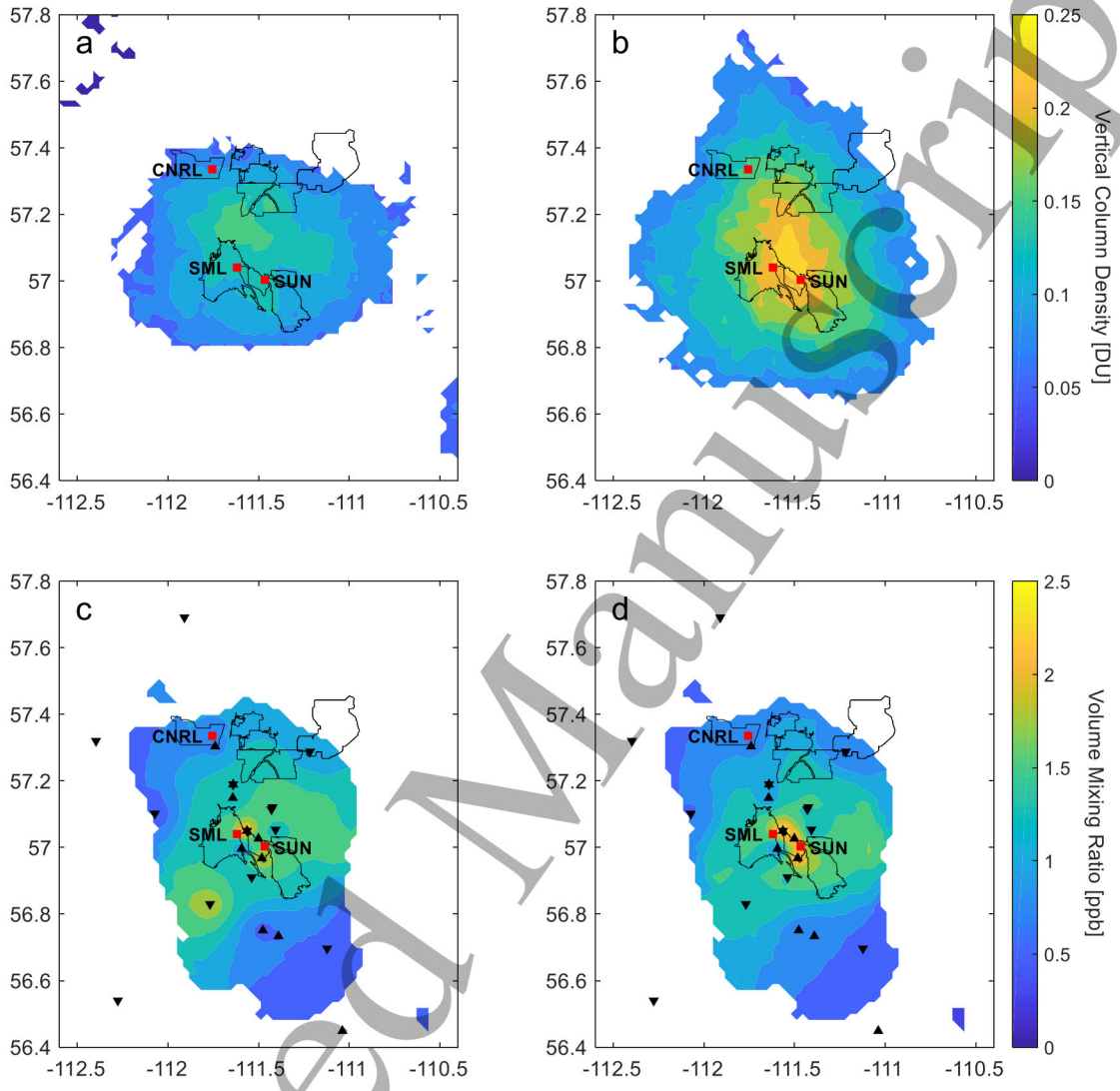

Figure 3: Multi-year average SO_2 for two four-year periods over the surface mines (outlined in black): (a) 2010-2013 and (b) 2014-2017 April-October OMI vertical column densities (in Dobson Units); (c) 2010-2013 and (d) 2014-2017 WBEA volume mixing ratios from continuous and passive observations. The red squares indicate the location of the upgraders. In (a) and (b) only locations in which the average VCD is at least 3 times larger than the standard error of the mean are shown. The locations of continuous (Δ) and passive (∇) observations are indicated in (c) and (d).

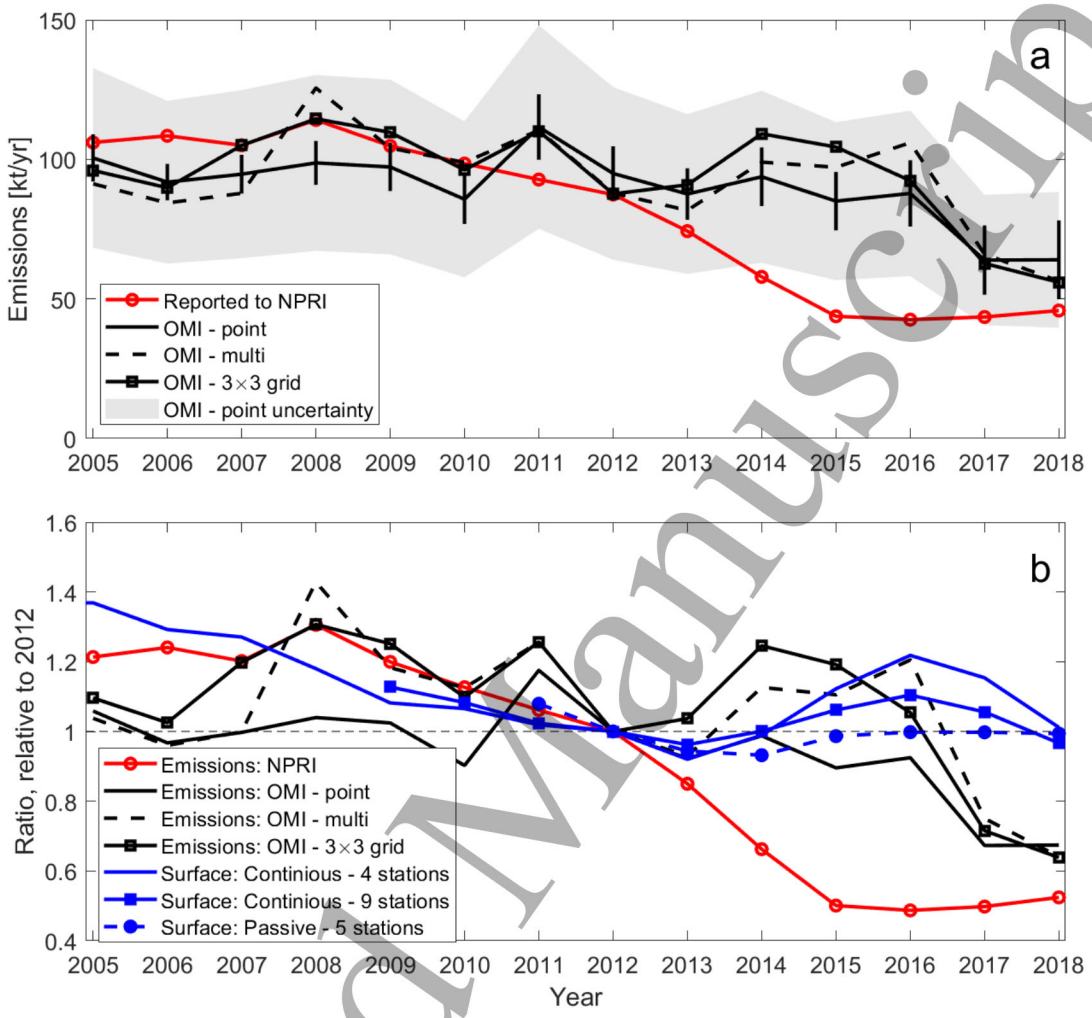

Figure 4: (a) Annual 3-year running mean SO_2 emissions from OMI and NPRI. (For example: OMI data from 2008-2010 were used to determine OMI 2009 emissions whereas for NPRI 2009 emissions, 2008-2010 values were simply averaged.) The black lines represent three different variations of emissions algorithms applied to OMI, with the grey shading indicating the total estimated uncertainty for the point source method and the error bars the variability. (b) Variation of annual emissions from panel (a) and 3-year mean surface concentrations (adapted from Figure 2), all relative to their value in 2012.

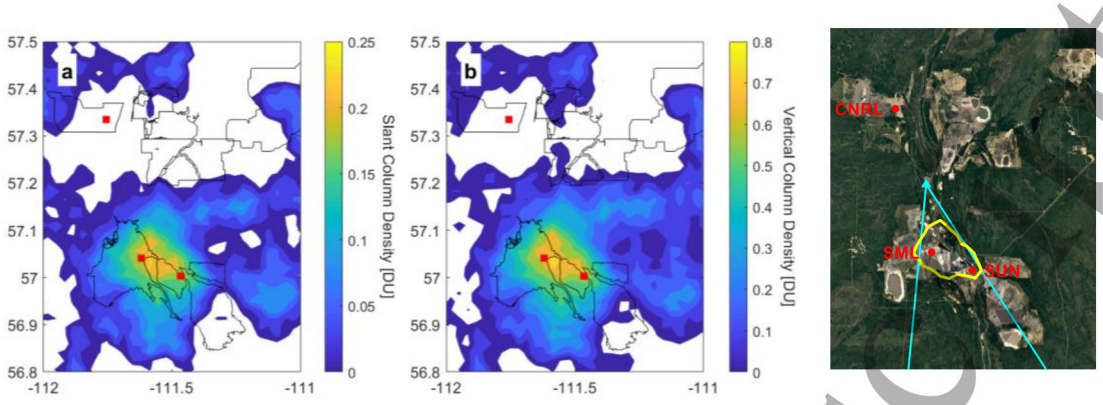

Figure 5: (a) April-October 2018 average TROPOMI SO_2 slant column density over the surface mines (outlined in black). White indicates SCDs that are slightly negative. The red squares are the location of the upgraders. (b) Same as (a) except showing VCDs. (c) True colour image showing estimated location of SO_2 emissions according to TROPOMI (yellow polygon) and Pandora (blue lines). The TROPOMI outline represents the contour corresponding to 75% of the peak SO_2 VCD.

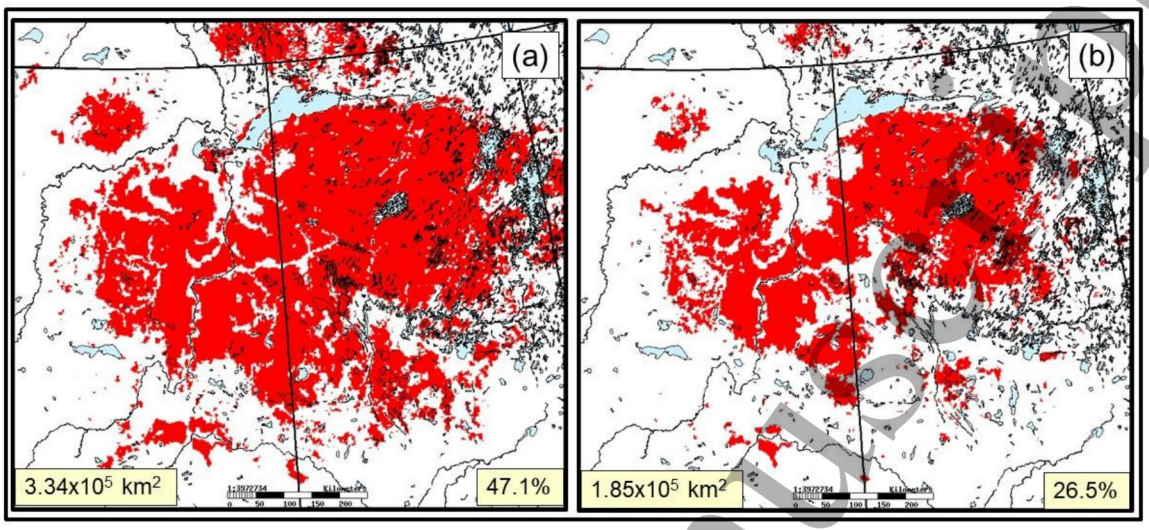

Figure 6: (a) Area in exceedance of aquatic critical loads using 2013 emissions data (from Makar et al., 2018). (b) Area in exceedance assuming all SO_2 emissions in the region are reduced by 40% (equivalent to the reported reduction between 2013 and 2016), and that SO2 concentrations and hence deposition fluxes scale linearly with SO2 emissions. Areas on the figure are the area in exceedance, percentages are the percent of the total area of aquatic ecosystems for which critical loads were available that is estimated to be in exceedance and are based on observation-corrected model output.